available at www.sciencedirect.com

SCIENCE DIRECT®

www.elsevier.com/locate/brainres

BRAIN RESEARCH

Research Report

Regional neuropathology following kainic acid intoxication in adult and aged C57BL/6J mice

*Stanley Anthony Benkovic, James Patrick O'Callaghan, Diane Bemis Miller**

Toxicology and Molecular Biology Branch, Centers for Disease Control and Prevention-National Institute for Occupational, Safety and Health, Mailstop 3014, 1095 Willowdale Road, Morgantown, WV 26505, USA

ARTICLE INFO

Article history:
Accepted 6 November 2005
Available online 5 January 2006

Keywords:
Age factor
Excitotoxicity
Gliosis
Neuropathology

ABSTRACT

We evaluated regional neuropathological changes in adult and aged male mice treated systemically with kainic acid (KA) in a strain reported to be resistant to excitotoxic neuronal damage, C57BL/6. KA was administered in a single intraperitoneal injection. Adult animals were dosed with 35 mg/kg KA, while aged animals received a dose of 20 mg/kg in order to prevent excessive mortality. At time-points ranging from 12 h to 7 days post-treatment, animals were sacrificed and prepared for histological evaluation utilizing the cupric-silver neurodegeneration stain, immunohistochemistry for GFAP and IgG, and lectin staining. In animals of both ages, KA produced argyrophilia in neurons throughout cortex, hippocampus, thalamus, and amygdala. Semi-quantitative analysis of neuropathology revealed a similar magnitude of damage in animals of both ages, even though aged animals received less toxicant. Additional animals were evaluated for KA-induced reactive gliosis, assayed by an ELISA for GFAP, which revealed a 2-fold elevation in protein levels in adult mice, and a 2.5-fold elevation in aged animals. Histochemical evaluation of GFAP and lectin staining revealed activation of astrocytes and microglia in regions with corresponding argyrophilia. IgG immunostaining revealed a KA-induced breach of the blood–brain barrier in animals of both ages. Our data indicate widespread neurotoxicity following kainic acid treatment in C57BL/6J mice, and reveal increased sensitivity to this excitotoxicant in aged animals.

* *Corresponding author*. Fax: +1 304 285 5708.
E-mail address: dum6@cdc.gov (D.B. Miller).

0006-8993/$ – see front matter © 2005 Elsevier B.V. All rights reserved.
doi:10.1016/j.brainres.2005.11.065

Abbreviations:
ABC, avidin–biotin complex
ah, alveus hippocampi
amyg, amygdala
ANOVA, analysis of variance
atc, area transitionalis corticoamygdaloidea
BCA, bicinchoninic acid
CA1, cornu ammonis region 1
CA3, cornu ammonis region 3
ccac, cortex cerebri, area cinguli
CDC, Centers for Disease Control and Prevention
cn, caudate nucleus
DAB, 3–3′ diaminobenzidine tetrahydrochloride
DPBS, Dulbecco's modified phosphate buffered saline
ectx, entorhinal cortex
EEG, electroencephalogram
ELISA, enzyme-linked immunosorbent assay
fctx, frontal cortex
GFAP, glial fibrillary acidic protein
hfd, hilus fasciae dentatae
hip, hippocampus
HRP, horseradish peroxidase
i.e., id est
IgG, immunoglobulin G
III, cortex cerebri, layer III
i.p., intraperitoneal
IsoB4, *Griffonia simplicifolia* isolectin B4
KA, kainic acid
lpeae, lamina principalis externa areae entorhinalis
lpiae, lamina principalis interna areae entorhinalis
nab, nucleus amygdaloideus basalis
nac, nucleus amygdaloideus corticalis
nah, nucleus anterior hypothalami
nam, nucleus amygdaloideus medialis
nat, nucleus anteroventralis thalami
NIOSH, National Institute for Occupational Safety and Health
nlh, nucleus lateralis hypothalami
nls, nucleus lateralis septi
nms, nucleus medialis septi
npt, nucleus paratenialis thalami
npvt, nucleus paraventricularis thalami
nrt, nucleus reticularis thalami
NSA, NeuroScience Associates
nts, nucleus triangularis septi
nvh, nucleus ventricularis hypothalami
nvtpa, nucleus ventralis thalami,

pars anterior
nvtpd, nucleus ventralis thalami, pars dorsalis
PBS, phosphate buffered saline
ps, parasubiculum
rcc, radiatio corporis callosi
RT, room temperature
scc, splenium corporis callosi
SDS, sodium dodecyl sulfate
SEM, standard error of the mean
sl-m, stratum lacunosum-moleculare hippocampi
smaid, stratum moleculare areae interna dentatae
so, stratum oriens hippocampi
sp, stratum pyramidale hippocampi
sps, stratum pyramidale subiculi
sr, stratum radiatum hippocampi
tcc, truncus corporis callosi
thal, thalamus
VI, cortex cerebri, layer VI

1. Introduction

Mice are increasingly utilized in experiments evaluating transgenesis and as animal models of disease, and our laboratory uses such models to investigate the ability of stressors to alter neurotoxicity of compounds that target the hippocampus. Kainic acid (KA) is a frequently utilized neurotoxicant that mimics the amino acid neurotransmitter glutamate and activates ionotropic glutamate receptors causing a cascade of intracellular events including: dysregulation of glutamate neurotransmission; disruption of calcium signaling; alteration of membrane electrophysiology; and generation of oxygen radicals (reviewed in (Ben-Ari and Cossart, 2000; Skaper et al., 1999; Wang et al., 2005)). Historical evaluation of kainic acid-induced neuropathology was generally performed in rat brain (Olney et al., 1979; Schwob et al., 1980; Sperk et al., 1983; Wuerthele et al., 1978); therefore, the consequences of KA intoxication in mouse brain are not completely described. As a precursor to stress studies, we characterized the basal response of several murine strains to KA by evaluating hippocampal homogenates for the induction of reactive gliosis with an ELISA for glial fibrillary acidic protein (GFAP). We used strains of mice reported to be "sensitive" and "resistant" to KA-induced excitotoxicity; however, GFAP levels were elevated in all mice, suggesting all strains exhibited glial activation, most likely in response to neuronal damage (Benkovic et al., 2000). Before proceeding with proposed stress studies, we initiated a characterization of the "resistant" strain, C57BL/6, using multiple indicators of neuronal damage and gliosis, to determine whether this commonly used strain was sensitive to KA-induced excitotoxic neuronal damage.

C57BL/6 mice were initially reported to be "resistant" to excitotoxic damage to hippocampal pyramidal neurons induced by systemic treatment with KA, in animals that displayed severe behavioral seizures (Schauwecker and Steward, 1997). Our laboratory recently reported the magnitude and time-course of neuropathological changes in hippocampus of C57BL/6J mice treated systemically with high dosages of KA (Benkovic et al., 2004). A battery of histological stains revealed extensive neuronal damage, activation of microglia and astrocytes, and disruption of the blood–brain barrier, in animals which displayed minimal behavioral seizure activity (i.e., Racine stage 1). Our conclusions emphasized the requirement of sensitive indicators of histological damage to be evaluated over a time-course both proximal and distal to treatment, because neuropathological effects of KA treatment were both underestimated by classical Nissl staining, and observed temporally with specialized staining techniques.

Descriptions of KA-induced seizure activity in mice are inconsistent, primarily due to differences in seizure scoring among laboratories. Several investigations have reported tonic–clonic seizures in mice treated with high dosages of KA (Chen et al., 2002; Hu et al., 1998; Santos and Schauwecker, 2003; Schauwecker, 2003; Schauwecker and Steward, 1997; Yang et al., 2005); however, seizures of this severity have not been observed in all evaluations (Araki et al., 2002; Benkovic et al., 2004; Chen et al., 2004a,b; Ferraro et al., 1995; Royle et al., 1999; Sriram et al., 2002). Interestingly, some evaluations report severe seizure activity following systemic injection of KA, with no concomitant neuropathology (Araki et al., 2002; Schauwecker, 2002, 2003; Schauwecker and Steward, 1997; Yang et al., 2005). In rat brain, severe seizure activity following KA administration is both positively correlated with and required for neuropathology (Schwob et al., 1980; Zhang et al., 1998); however, in mice, the correlation may not be as strict (Benkovic et al., 2004). Recent measurements of EEG activity of neurons in KA-treated mice indicate the animals reach a state of non-convulsive status epilepticus (Arabadzisz et al., 2005; Mazarati et al., 2004), suggesting an existent disconnection of electrical activity and behavioral seizures in mice.

The astrocyte and microglia response to neuronal damage is a generic process termed "reactive gliosis" that may involve

the production of growth factors and cytokines. In rats and mice, elevated GFAP levels, a hallmark of astrogliosis, have been reported following various types of neural injury (Eng et al., 1969; Little and O'Callaghan, 2002; Norenberg, 1994; O'Callaghan, 1993; O'Callaghan and Miller, 1994; Panickar and Norenberg, 2005; Petzold et al., 2003). In adult C57BL/6J mice, we reported the time-course and magnitude of induction of GFAP following KA intoxication, which resulted in a peak three-fold elevation in protein levels at 7 days post-treatment (Benkovic et al., 2004); however, the magnitude of GFAP elevation in aged mice has not been determined.

Age is a risk factor that can impact neurotoxicity caused by several classes of compounds. In case reports of human poisoning following ingestion of mussels containing the marine algal toxin domoic acid, elderly individuals were the greatest affected suggesting an age-related supersensitivity to excitotoxins (Perl et al., 1990). In rats, age-related exacerbation of neurotoxicity has been observed following intoxication with D-amphetamine (Bowyer et al., 1998; Sankar et al., 1983), methamphetamine (Imam and Ali, 2001), trimethyltin (Scallet et al., 2000), 6-hydroxydopamine (Cass et al., 2005), and kainic acid (Dawson and Wallace, 1992; Wozniak et al., 1991). In mice, age affects the susceptibility to the dopaminergic neurotoxicity of methamphetamine (Miller et al., 2000); however, the effects of excitotoxins have not been fully investigated in aged animals.

Here, we expand our previous report of hippocampal pathology, and characterize regional argyrophilia, activation of glial cells, and breach of the blood–brain barrier in adult and aged C57BL/6J mice treated systemically with KA. We observed similar levels of KA-induced argyrophilia in brains of adult and aged animals, even though the aged animals received a lower dose of toxicant. Brain regions displaying argyrophila also showed activation of both astrocytes and microglia. Our data indicate widespread neuronal damage in the brains of KA-treated C57BL/6J mice, that damage is observed following mild behavioral seizure activity, and aged animals appear more sensitive to the effects of this excitotoxicant.

2. Results

2.1. Seizure scoring

KA treated animals displayed behavioral seizures that segregated into two categories: mild and severe. Within 15 min of injection, all animals displayed stage 1 seizures (mouth and facial movements). Over the next 30 min, approximately 35% of treated animals displayed progressive seizures: 10% peaked at stage 2; while 25% experienced severe tonic–clonic seizures followed by death of the animal. No surviving animals peaked between stages 3 and 5. Aged animals treated with a lower dose of KA displayed similar seizures that could also be segregated into "mild" and "severe" groups. Mortality was approximately 50% in the aged group. During the survival period, the mice showed no residual effects of treatment (i.e., no obvious seizure or behavioral effects). All histological data presented here is from animals displaying behavioral seizures of stages 1–2. No seizure activity was observed in animals treated with saline.

2.2. Quantification of hippocampal GFAP by ELISA

KA treatment (20 mg/kg) caused an elevation in hippocampal GFAP levels at 7 days post-treatment (Fig. 1). Adult animals showed a two-fold increase in protein levels compared to saline-injected controls. Aged animals showed a significant 2.5-fold elevation. GFAP levels in adult and aged saline-injected controls were not statistically different, i.e., no age-related increase in protein levels was observed.

2.3. Overview of kainic acid-induced regional pathology

Low-magnification whole-brain imaging revealed KA treatment of both adult and aged animals resulted in neuronal damage (Figs. 2A, B), astroglial (C, D) and microglial (E, F) activation, and disruption of the blood–brain barrier with subsequent influx of plasma-derived IgG (G, H). Each stain revealed an increased sensitivity of aged animals to treatment, though they received a lower dose of toxicant. All subsequent regional pathology was recorded from time-points corresponding to the peak of argyrophilia: 24 h post-treatment in adult animals; and 3 days post-treatment in aged animals.

2.4. Cupric-silver neurodegeneration stain

Both adult and aged mice treated with KA displayed treatment-induced argyrophilia compared to saline-injected

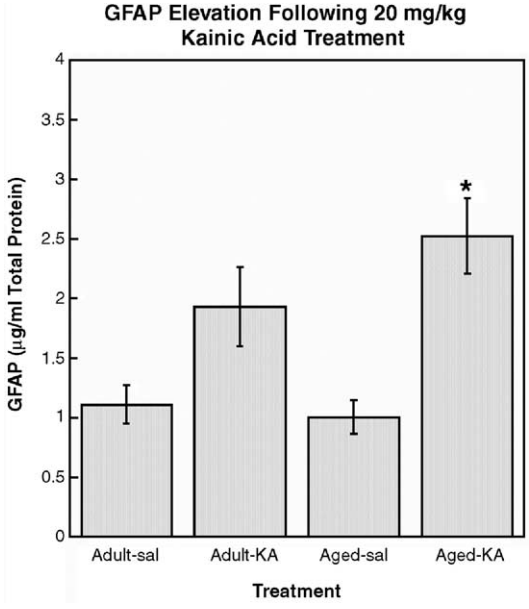

Fig. 1 – KA-induced GFAP levels in adult and aged mice. Adult and aged mice received an intraperitoneal injection of saline or 20 mg/kg KA. Seven days following treatment, hippocampi were removed and assayed for GFAP levels by ELISA. KA treatment caused a near-significant two-fold elevation in GFAP in adult animals, and a significant 2.5-fold elevation in protein levels in aged mice (asterisk), when compared to the corresponding age-matched saline-injected controls.

controls (data not shown as virtually no signal is present). An overview of the regional distribution and magnitude of argyrophilia revealed increased deposition of silver onto cell bodies and processes in aged animals, though they were dosed with less toxicant (Figs. 2A, B). Regional neuronal populations susceptible to KA-induced excitotoxic damage, and the comparison of the intensity, distribution, and time-course of argyrophilia in adult and aged animals follows.

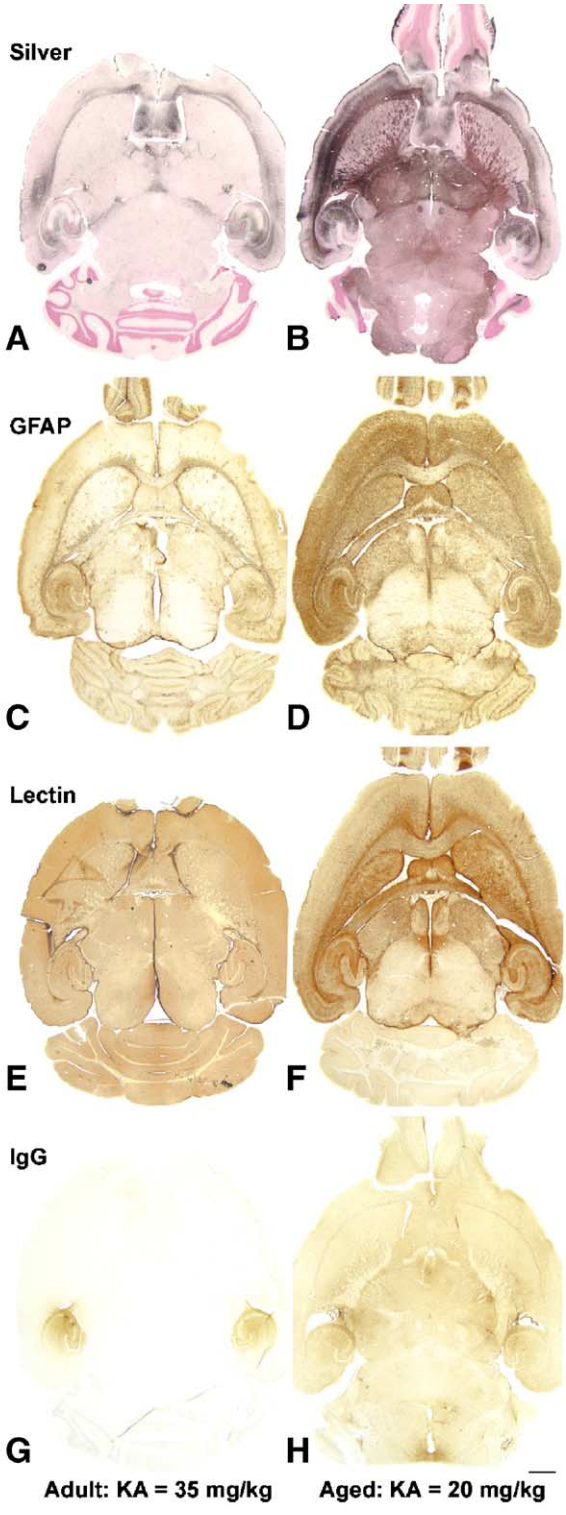

2.5. *Hippocampus*

By 12 h following KA treatment of adult mice, argyrophilic fibers were observed in stratum oriens and stratum lacunosum-moleculare, and a few silver-stained neurons were observed in CA3 of stratum pyramidale hippocampi. Occasional argyrophilic neurons and interneurons were observed in CA1 and stratum oriens, respectively. Mild fiber staining was detected in stratum pyramidale subiculi. Several animals displayed loss of Nissl counterstaining in subregion CA3 (arrow in Fig. 3C); however, these neurons were not argyrophilic. By 24 h post-injection, severely damaged neuronal processes were observed in all hippocampal strata, and argyrophilic neurons were evident in all subregions of stratum pyramidale hippocampi, stratum pyramidale subiculi, and both interna and externa components of the lamina principalis presubiculi (Figs. 3A, C). At high magnification, complete silver-stained neurons could be distinguished, with the cell body embedded in the pyramidal layer, basilar dendrites extending into stratum oriens, and the apical dendrite coursing through stratum radiatum as far as fissura hippocampi. The parasubiculum was relatively spared (Fig. 3C). Damaged neurons within the laminal principalis interna areae entorhinalis were observed along with their argyrophilic terminal projections in the fasciae dentatae (Fig. 3C). In severely affected animals, a band of argyrophilic fibers was observed in fasciae dentatae, moleculare interna, resulting from damage to neurons in the contralateral polymorphic layer of the dentate gyrus (Figs. 3A, C). In the hilus of some animals, an abrupt transition was observed between damaged fibers in stratum radiatum and an undamaged polymorphic layer (see effect in aged animal in Fig. 3D). By 3 days post-injection, argyrophilia was attenuated; however, residual fiber staining was observed in hippocampal strata and occasional neurons were evident in stratum pyramidale hippocampi. By 7 days post-treatment, the hippocampus appeared similar to saline-injected controls.

In aged animals viewed at 12 h post-injection, KA treatment resulted in argyrophilia throughout the hippocampus

Fig. 2 – Overview of KA-induced pathology in adult and aged mice revealed by GFAP immunohistochemistry, cupric-silver staining, lectin staining, and IgG immunohistochemistry. Adult animals (A, C, E, G) were treated with 35 mg/kg KA while aged animals were dosed at 20 mg/kg (B, D, F, H). KA treatment caused the appearance of argyrophilic neurons throughout the brain in animals of both ages (A, B); however, aged animals displayed a greater response to toxicant treatment. Neuronal damage resulted in the activation of astrocytes and microglia throughout the brain of adult (C, E) and aged (D, F) mice, in regions with corresponding argyrophilia. Aged animals displayed a greater intensity of GFAP immuno- and lectin staining, and a more thorough regional pattern of activation. In adult mice, KA treatment caused a breach of the BBB that was restricted to the hippocampus (G). In aged animals treated with KA, breach of the barrier was observed in all circumventricular regions, and a low-level immunoreactivity was observed throughout the parenchyma (H). Bar = 2000 μm.

Fig. 3 – Regional comparison of argyrophilia I. Adult animals (A, C, E) were treated with 35 mg/kg KA while aged animals were dosed at 20 mg/kg (B, D, F). KA caused damage to the hippocampus and the appearance of argyrophilic neurons in stratum oriens hippocampi and stratum pyramidale hippocampi (A, B). Silver deposition onto damaged fibers was observed in stratum oriens hippocampi, stratum radiatum hippocampi, and stratum lacunosum-moleculare hippocampi (A, B). In aged animals, silver-stained fibers were observed in several white matter tracts including radiato corporis callosi, splenium corporis callosi, truncus corporis callosi, and alveus hippocampi (B). In caudo-ventral hippocampus, argyrophilic neurons were observed in lamina principalis externa presubiculi, lamina principalis interna presubiculi, and stratum pyramidale subiculi (C, D). In some animals, damaged terminals of hilar neurons were observed in the contralateral projection field, stratum moleculare areae interna dentatae (C). Parasubiculum was relatively spared in animals of both ages (C, D). KA caused the appearance of argyrophilic neurons in cortex cerebri, areae cinguli, and in nuclei triangularis and lateralis septi (E, F). Scale bar = 500 μm.

and lamina principalis, areae entorhinalis. The magnitude of the argyrophilic reaction appeared maximal by 24 h post-treatment, but remained elevated through 3 days post-injection. KA caused the appearance of argyrophilic neurons in all subregions of stratum pyramidale hippocampi, and the deposition of silver onto fibers in stratum oriens hippocampi, stratum radiatum hippocampi, and stratum lacunosum-moleculare (Figs. 3B, D), radiato corporis callosi, splenium corporis callosi, and truncus corporis callosi (Fig. 3B). A few argyrophilic neurons were observed in stratum griseum superficiale colliculi anterioris and stratum griseum mediale colliculi anterioris (Fig. 3B). Neurons appeared damaged in lamina principalis externa presubiculi and lamina principalis interna presubiculi (Fig. 3D); however, the parasubiculum was relatively spared (Fig. 3D). At 7 days post-treatment, a higher percentage of aged animals displayed persistent argyrophilia

when compared to adult animals. Argyrophilic neurons remained visible in stratum pyramidale hippocampi and stratum pyramidale subiculi, and silver-stained fibers were apparent in all hippocampal strata. Mild argyrophilia of polymorphic neurons and fibers was observed in the hilus and fasciae dentatae.

2.6. Cerebral cortex

All four subdivisions of cerebral cortex displayed KA-induced argyrophilia, although with considerable variability of magnitude and time-course. At 12 h post-treatment, argyrophilic neurons were observed throughout the lamina of cortex cerebri, area temporalis (mainly II, III, and VI), occasionally in occipitalis (III, VI), and only in VI of parietalis. In cortex cerebri, area frontalis, argyrophilic neurons were apparent in lamina VI and throughout area cinguli. By 24 h post-treatment, the quantity of silver-stained neurons and fibers in temporalis was increased in cortical layers III–VI, and a few stained cells and fibers were detected in the caudal region of parietalis (Fig. 3C). Cortex cerebri, area temporalis and area occipitalis had many damaged neurons including some intensely argyrophilic cells in lamina III that extended apical processes to lamina I (Fig. 3C). Damage to cortex cerebri, areae frontalis most consistently involved the cortex cerebri, areae cinguli (Fig. 3E). A consistent band of intensely argyrophilic neurons was observed in neocortical layer VI throughout all lobes (Figs. 3A, C, E), and this band extended into layer III in the most severely affected animals. Fibers in corporis callosi were spared (Fig. 3E). By 3 days post-treatment, argyrophilia was attenuated in all cortical regions; however, some residual staining was observed in cells and processes in cortex cerebri, area temporalis and area occipitalis. At 7 days post-injection, argyrophilia in neocortical layer VI of most animals had resolved, and only one animal displayed minimal silver-staining in cortex cerebri, area temporalis layers III and VI.

In aged animals viewed at 12 h post-treatment, argyrophilia began to appear in neurons of neocortical layer VI. No other cortical layers appeared argyrophilic. By 24 h post-injection, argyrophilic neurons were observed in cortex cerebri, area occipitalis, and in cortex cerebri, area cinguli. By 3 days post-treatment, neuronal damage was observed in all four cerebral cortical regions. Silver deposition onto fibers was observed in radiatio corporis callosi, truncus corporis callosi, splenium corporis callosi, and alveus hippocampi (Fig. 3B). Cerebral cortex, area parietalis displayed occasional damaged neurons; however, in extreme cases argyrophilic neurons were observed throughout layers III–VI. Damage in cortex cerebri, area occipitalis and area temporalis was observed in layers III–VI (Fig. 3D). In cortex cerebri, area entorhinalis, severe KA-induced argyrophilia was observed in lamina principalis externa areae entorhinalis and lamina principalis interna areae entorhinalis (Fig. 3D). Cortex cerebri, area cinguli was affected in all animals (Fig. 3F). At 7 days post-treatment, argyrophilia appeared attenuated; however, silver stained cells and fibers remained evident in all four cerebral cortical regions.

2.7. Thalamus/septum

Adult mice treated with KA began to show argyrophilia in thalamic nuclei as early as 12 h post-injection, and many nuclei were distinctly demarcated from surrounding unaffected regions. Nucleus lateralis habenulae contained silver-stained cells and processes, but nucleus medialis habenulae was unaffected. Rostral thalamic nuclei including lateralis, posterior, and ventralis were unaffected, but sharply demarcated from caudal nuclei by an argyrophilic band of neurons that contained nucleus pretectalis profundus. By 24 h, argyrophilic neurons were observed in: nucleus lateralis thalami; nucleus lateralis thalami, pars posterior; nucleus paraventricularis thalami; and nucleus medialis thalami, pars lateralis. In more ventral sections, argyrophilic neurons were observed in: nucleus ventralis thalami, pars anterior; and nucleus ventralis thalami, pars dorsalis (Fig. 4A), while nucleus rhomboideus thalami and nucleus paratenialis thalami were relatively spared. Silver-stained neurons and fibers were observed in nucleus triangularis septi, nucleus lateralis septi, and nucleus medialis septi (Fig. 4A). At 3 and 7 days post-treatment, argyrophilia was attenuated nearly to control levels; however, residual staining of some cells and processes was observed in nucleus pretectalis profundus.

Aged mice injected with kainic acid and viewed at 12 h post-treatment began to show silver deposition onto fibers in stria medullaris thalami and fasciculus longitudinalis medialis, and in more ventral sections, fasciculus retroflexus. By 24 h post-treatment, an argyrophilic band of neurons was distinctly observed that included nucleus pretectalis profundus. Occasional silver-stained neurons were scattered through caudal thalamic cranial nerve nuclei including nucleus nervii oculomotorii, and nucleus nervii trochlearis. By 3 days post-treatment, a severe argyrophilic reaction was observed in: nucleus lateralis thalami; nucleus medialis thalami, pars lateralis; nucleus ventralis thalami, pars lateralis; and nucleus paraventricularis thalami. Severely affected animals displayed argyrophilia in nucleus dorsalis corporis geniculati lateralis. In ventral thalamus, KA-induced argyrophilia was observed in nucleus paratenialis thalami, nucleus anteromedialis thalami, nucleus reticularis thalami, and nucleus paraventricularis thalami (Fig. 4B). Damaged neurons were observed in nucleus lateralis septi, nucleus medialis septi, and nucleus triangularis septi (Fig. 4B). Argyrophilic fibers were observed in the fasciculus retroflexus (Fig. 4B), and silver deposition onto damaged thalamic radiations coursing through nucleus caudatus (Fig. 4B) and into the olfactory bulb were observed.

2.8. Hypothalamus

By 12 h following KA treatment of adult mice, mild argyrophilia of cells and processes was observed in nucleus supramammillaris, and scattered silver-stained neurons were observed in nucleus ventromedialis hypothalami and nucleus lateralis hypothalami. By 24 h post-injection, mild argyrophilia appeared in nucleus anterior hypothalami, nucleus dorsomedialis hypothalami, and nucleus posterior hypothalami. The magnitude of argyrophilia increased slightly in nucleus ventromedialis hypothalami, and a few silver-

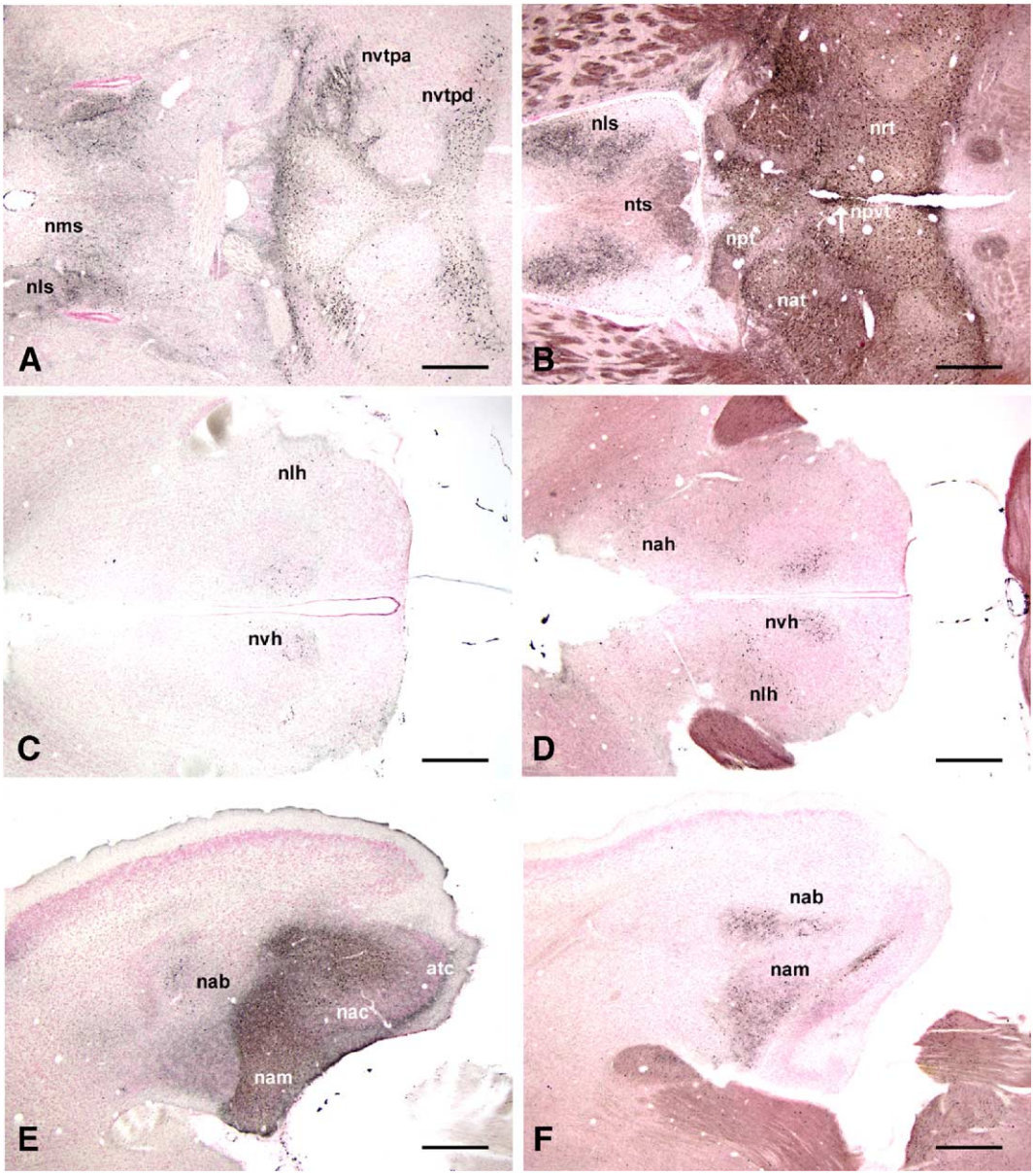

Fig. 4 – Regional comparison of argyrophilia II. Adult animals (A, C, E) were treated with 35 mg/kg KA while aged animals were dosed at 20 mg/kg (B, D, F). KA caused the appearance of argyrophilic neurons in several thalamic nuclei including: nucleus ventralis thalami, pars anterior and dorsalis (A); nucleus paratenialis thalami, nucleus reticularis thalami, nucleus anteromedialis thalami, and nucleus para ventricularis thalami (B). In hypothalamus, a few scattered argyrophilic neurons were observed in nucleus lateralis hypothalami and nucleus ventromedialis hypothalami (C, D). Argyrophilic neurons were observed in amygdaloid areas including nucleus amygdaloideus lateralis, and nucleus amygdaloideus medialis (E, F). Scale bar = 500 μm.

stained neurons were observed in nucleus mammillaris lateralis (Fig. 4C). By 3 days post-treatment, argyrophilia was no longer observed in the hypothalamus.

In aged mice, KA-induced damage was first observed in fibers. By 12 h post-treatment, argyrophilic fibers were observed in tractus opticus and crus cerebri. A few argyrophilic neurons were scattered through nucleus paraventricularis hypothalami, nucleus ventromedialis hypothalami, and nucleus lateralis hypothalami. By 24 h post-injection, the magnitude of argyrophilia increased slightly, and additional silver-stained cells and processes were observed in nucleus anterior hypothalami, zona incerta, nucleus preopticus medialis, and nucleus periventricularis arcuatus hypothalami. By 3 days post-treatment, argyrophilia was attenuated nearly to control levels; however, a few silver-stained neurons were observed in nucleus anterior hypothalami, nucleus ventromedialis hypothalami, and nucleus lateralis hypothalami (Fig. 4D). Fiber staining was persistent through 7 days post-injection in tractus opticus and crus cerebri.

2.9. *Amygdala*

At 12 h following KA treatment, argyrophilia in amygdala was limited to minimal staining of a few cells and processes in nucleus amygdaloideus lateralis, pars posterior. By 24 h post-injection, mild argyrophilia was observed in: nucleus amygdaloideus centralis; nucleus amygdaloideus basalis, pars medialis; and nucleus amygdaloideus lateralis, pars posterior. Severe neuronal degeneration was observed in nucleus amygdaloideus medialis and nucleus amygdaloideus corticalis (Fig. 4E). The areae transitionalis corticoamygdaloidea contained a dense band of argyrophilic neurons (Fig. 4E). By 3 days post-treatment, argyrophilia was attenuated nearly to control levels; however minor residual staining was observed in nucleus amygdaloideus lateralis, pars posterior and nucleus amygdaloideus centralis.

In aged animals treated with KA and viewed at 12 h post-injection, argyrophilia was limited to a few silver-stained cells and processes in nucleus amygdaloideus corticalis and nucleus amygdaloideus lateralis, pars posterior. By 24 h post-treatment, argyrophilia was increased slightly and stained cells and processes were observed in: nucleus amygdaloideus centralis; nucleus amygdaloideus medalis; nucleus amygdaloideus basalis, pars medialis; and nucleus amygdaloideus basalis, pars lateralis (Fig. 4F). In most animals at 3 days following treatment, argyrophilia was attenuated to residual staining in nucleus amygdaloideus corticalis and nucleus amygdaloideus basalis, pars lateralis; however, one animal had persistent argyrophilia through 7 days post-injection in nucleus amygdaloideus corticalis and nucleus amygdaloideus basalis, pars lateralis.

2.10. *Pyriform cortex/olfactory nucleus*

At 12 h following KA treatment, argyrophilia was not evident in cortex cerebri, area pyriformis. By 24-h post-injection, a few argyrophilic neurons were observed in the lamina pyramidalis areae pyriformis, and silver-stained processes were apparent in lower cortical laminae. The nucleus tractus olfactorii lateralis was highly damaged, and was easily observed among the surrounding neuropil due to the intensity of argyrophilic neurons and fibers. By 3 days post-treatment, argyrophilia was attenuated to control levels.

In aged mice, KA intoxication caused the deposition of silver onto neurons and fibers of the nucleus tractus olfactorii lateralis by 12 h post-treatment. Damaged fibers were observed in tractus opticus. At 24 h post-injection, a few argyrophilic cells were observed in lamina pyramidalis areae pyriformis, and silver-stained processes and terminals were observed in cortex cerebri, area pyriformis. By 3 days post-treatment, argyrophilia was attenuated to residual fiber and terminal staining in lower layers of cortex cerebri, area pyriformis.

2.11. *Basal ganglia*

The nucleus caudatus/putamen of adult mice appeared to be relatively unaffected by kainic acid treatment (Fig. 2A). Argyrophilic neurons and processes were observed in nucleus accumbens septi at 24 h post-treatment only.

In aged animals, KA-induced argyrophilia in the nucleus caudatus/putamen was restricted to the fibers of passage (Figs. 2B, 3F, 4B), no argyrophilic neurons were observed. In nucleus accumbens septi, silver-stained neurons and processes were observed at 24 h post-treatment, and at 3 days post-treatment in one animal.

2.12. *Cerebellum*

KA-induced argyrophilia in the cerebellum was restricted to minor staining of granule cells and processes in one treated animal.

In aged animals, argyrophilia observed in the cerebellum was restricted to the white matter in animals treated with kainic acid.

2.13. *Semi-quantitative analysis of kainic acid-induced argyrophilia*

In adult C57BL/6J mice, treatment with KA caused significant argyrophilia in hippocampus, thalamus, cortex, and amygdala at 24 h post-treatment (Figs. 5A, B). Non-significant increases in argyrophilic neurons and fibers were observed in striatum, hypothalamus, and cerebellum.

In aged animals, KA treatment caused significant argyrophilia in hippocampus, thalamus, cortex, striatum, and amygdala at 3 days post-treatment (Figs. 5C, D). A non-significant elevation in argyrophilic neurons was observed in the hypothalamus.

2.14. *GFAP immunohistochemistry*

Intoxication of both adult and aged mice with KA resulted in an increase in GFAP immunoreactivity compared to saline-injected controls (data not shown). Elevated immunostaining for GFAP was observed in brain regions that displayed concomitant argyrophilia (Figs. 2A–D), and the time-course of astrocyte activation appeared as a response to neuronal damage. An overview of the regional distribution and magnitude of immunoreactivity revealed increased astrogliosis in aged animals, though they received a lower dose of toxicant (Figs. 2C, D).

In adult animals at 12 h post-treatment, GFAP immunoreactivity in hippocampus was only slightly elevated compared to saline-injected controls. In cortex cerebri, area frontalis and parietalis, GFAP immunoreactivity was generally restricted to layers I and VI. Elevated immunostaining was observed in cortex cerebri, area cinguli, cortex cerebri, area entorhinalis, and in rostral thalamus. At 24 h post-treatment, hippocampal immunoreactivity was exacerbated (Fig. 6C). Cortical regions began showing immunoreactivity in all layers (Figs. 6A, C, E), and staining was intensified in amygdala (Fig. 6E) and hypothalamus. By 3 days post-treatment, the hippocampus contained hypertrophied astrocytes that emanated processes swollen with the intermediate filament. Severe astrogliosis was observed throughout cortex and amygdala. At the latest time-point examined, 7 days post-treatment, astrocytes remained highly activated in

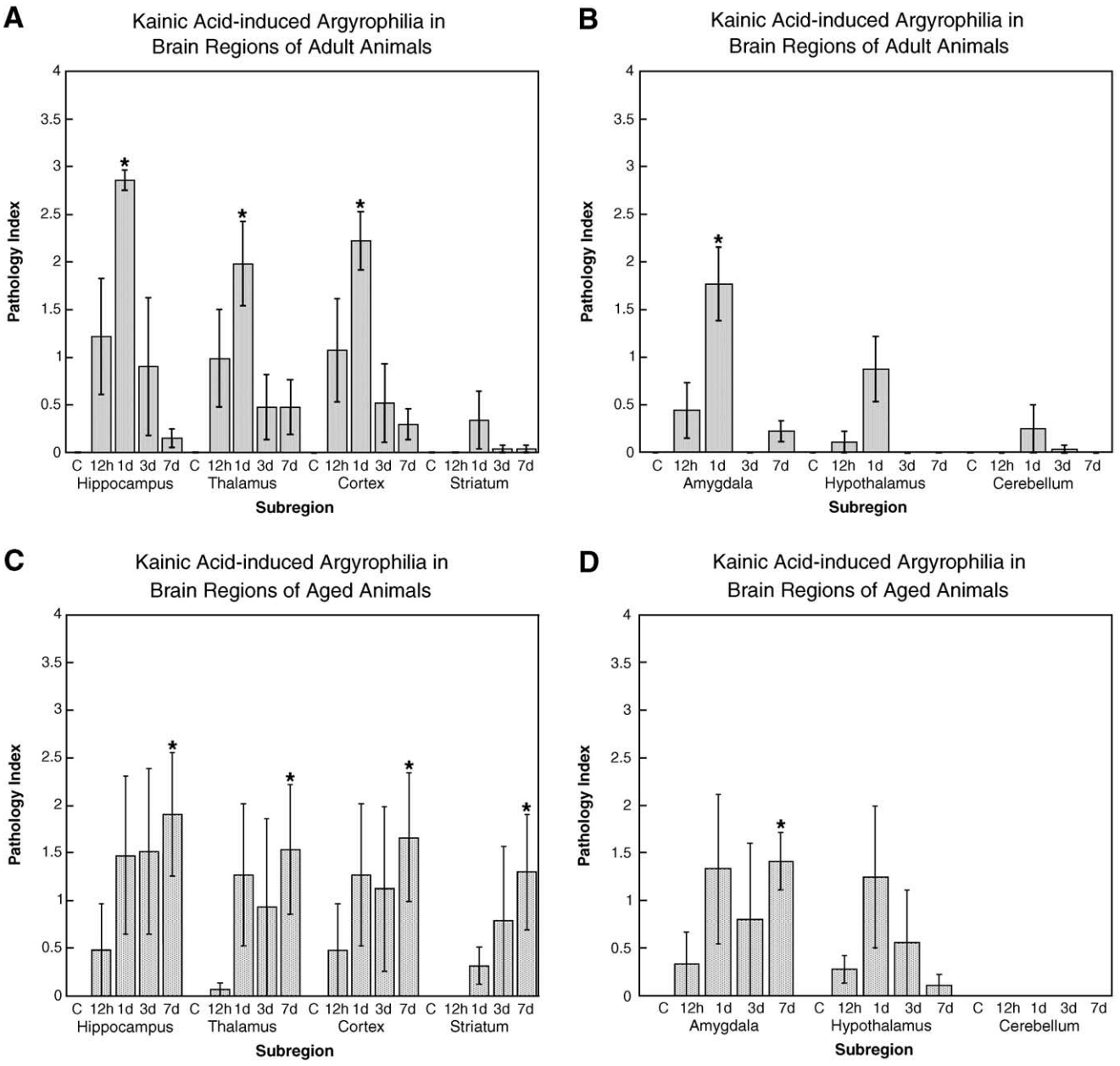

Fig. 5 – Semi-quantitative analysis of kainic acid-induced neuropathology. In adult C57BL/6J mice, kainic acid treatment caused a significant elevation in the quantity of argyrophilic neurons and fibers at 24 h post-treatment in hippocampus, thalamus, cortex, and amygdala (*$P = 0.026$, $P = 0.028$, $P = 0.028$, and $P = 0.028$, respectively). In aged animals, kainic acid treatment caused a significant elevation in the quantity of argyrophilic neurons and fibers at 7 days post-treatment in hippocampus, thalamus, cortex, striatum, and amygdala ($P = 0.037, 0.037, 0.037, 0.037, 0.037$, respectively).

all brain regions, even though argyrophilia was attenuated nearly to control levels.

Aged animals displayed a higher basal immunoreactivity for GFAP than adult mice. Saline-injected control animals showed staining in striatum and cortex that was not observed in adult control mice. The time-course of astrocyte activation following treatment was similar to adults; however, the intensity of the immunoreactivity was considerably greater at all time-points examined. Aged animals consistently displayed greater immunoreactivity for GFAP in brain regions including: cortex and striatum (Figs. 6B, D, F); hippocampus (Fig. 6D), and amygdala (Fig. 6F).

2.15. *Lectin histochemistry*

Treatment of both adult and aged mice with KA resulted in an increase in lectin stained cells compared to saline-injected controls indicating a toxicant-induced activation of microglia (data not shown). An overview of the regional distribution and magnitude of lectin staining revealed microgliosis in brain

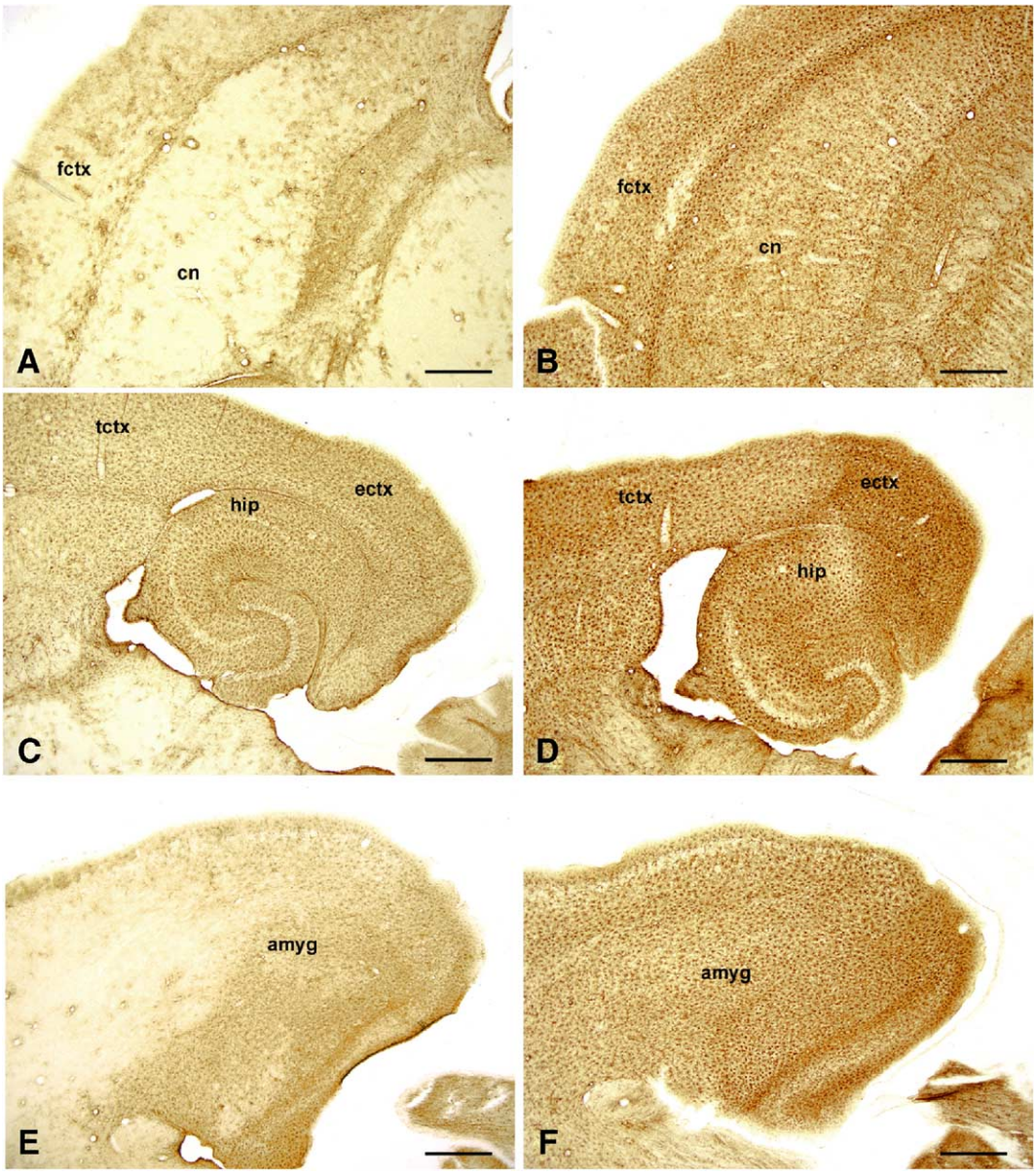

Fig. 6 – Comparison of astrogliosis in adult and aged mice revealed by GFAP immunohistochemistry. Adult animals (A, C, E) were treated with 35 mg/kg KA while aged animals were dosed at 20 mg/kg (B, D, F). Aged animals displayed a greater intensity and magnitude of astrogliosis compared to adult animals following treatment in frontal cortex and caudate nucleus (B vs. A), temporal and entorhinal cortices, hippocampus (D vs. C), and amygdala (F vs. E). Scale bar = 500 μm.

regions that displayed concomitant argyrophilia and thus, neuronal damage (Figs. 2A, B, E, F).

In adult animals at 12 h following treatment, processes of microglial cells began to appear in hippocampus and thalamus. A low-level microgliosis was observed in cortex cerebri, area occipitalis and entorhinalis, and in layer VI of all cortical regions. By 24 h post-injection, numerous profiles of microglia were observed in hippocampus, and staining was evident in processes and the cell soma (Fig. 7C). The intensity and magnitude of staining was increased in cortex cerebri, area occipitalis, especially in layer VI of all cortical regions (Fig. 7A), and in thalamus and septum (Fig. 7E). By 3 days post-treatment, brain-wide lectin staining was remarkably attenuated, although residual staining was observed in hippocampus, cortex, and thalamus. At 7 days post-treatment, microgliosis was further attenuated, but some residual lectin staining remained evident in hippocampus.

In aged animals, the intensity of basal lectin staining, and time-course of microglial activation and subsequent return to baseline was similar to adults. Compared to adult mice, aged animals displayed increased quantity and intensity of stained cells, though they received a lower dose of toxicant. Activated microglial cells were observed in all animals, and were especially apparent in cortex (Fig. 7B), hippocampus (Fig. 7D), and thalamus (Fig. 7F).

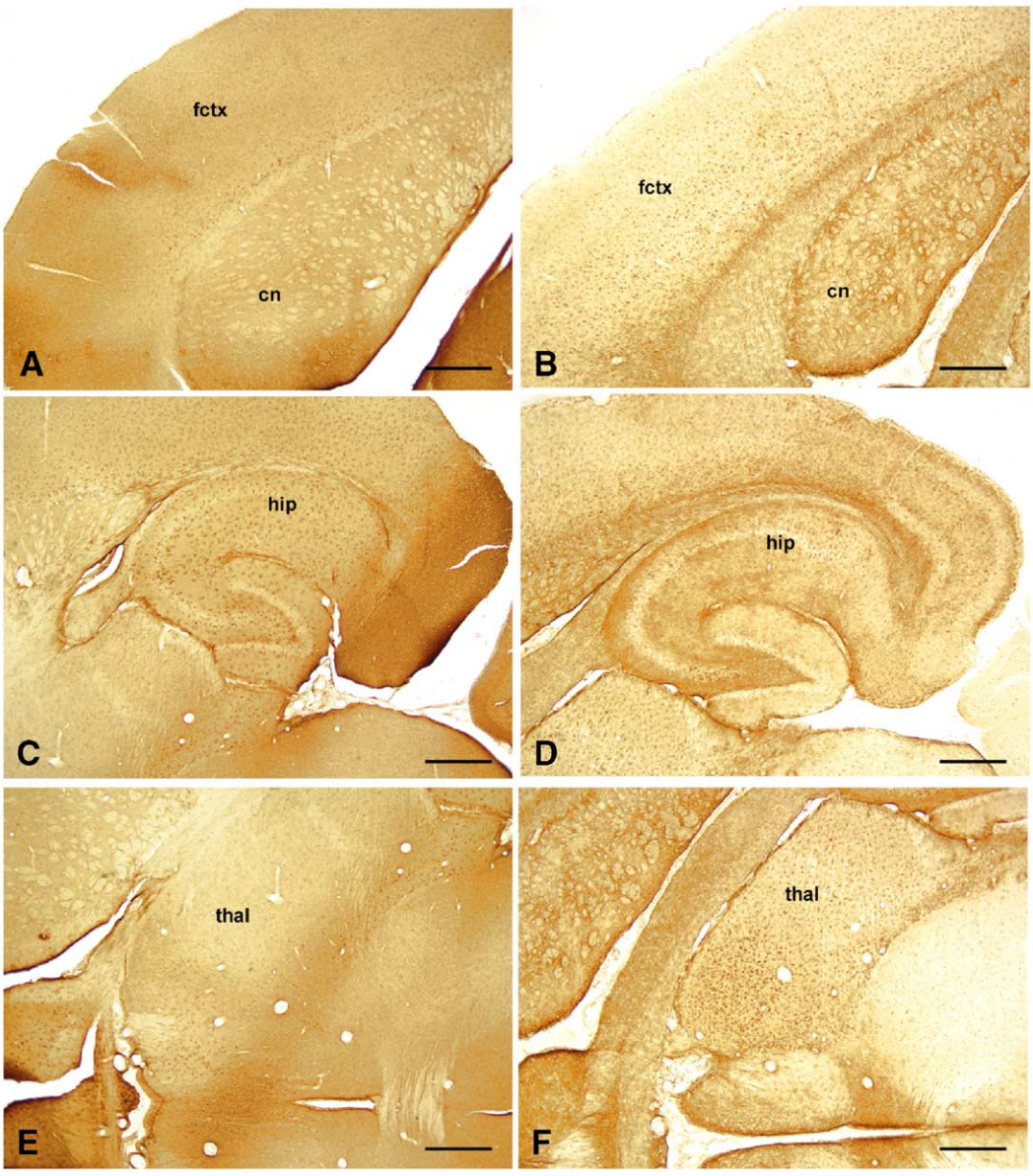

Fig. 7 – Comparison of microgliosis in adult and aged mice revealed by lectin staining. KA treatment caused the activation of microglia throughout the brain, in regions with corresponding argyrophilia. Aged animals displayed a greater intensity and magnitude of microgliosis compared to adult animals following treatment in frontal cortex and caudate nucleus (B vs. A), hippocampus (D vs. C), and thalamus (F vs. E). Scale bar = 500 μm.

2.16. *IgG immunohistochemistry*

Intoxication of both adult and aged mice with KA resulted in a breach of the blood–brain barrier, and an increase in IgG immunoreactivity compared to saline-injected controls (data not shown). An overview of the regional distribution and magnitude of immunoglobulin immunoreactivity revealed the susceptibility of the hippocampal BBB to breach in animals of both ages (Figs. 2G, H). Aged animals, which were treated with a lower dose of toxicant, displayed a low-level immunoreactivity throughout the parenchyma, and increased immunoglobulin immunoreactivity in all circumventricular regions (Fig. 2H).

In adult animals at 12 h post-treatment, considerable immunoreactivity for IgG was observed, yet was restricted to the hippocampus. By 24 h post-treatment, faintly immunoreactive microglia were observed throughout the hippocampal parenchyma. By 3 days post-injection, the integrity of the BBB was re-established, parenchymal IgG was no longer visible, and the hippocampus appeared similar to saline-injected control animals.

Aged animals showed a low-level basal staining for IgG suggesting an aged-related attenuation in barrier integrity. By 12 h post-treatment, IgG immunoreactivity was observed throughout the brain, and was especially evident in circumventricular regions. Immunoreactivity increased through

24 h and 3 days post-injection, and remained visible at the latest time-point examined, 7 days post-treatment.

3. Discussion

C57BL/6 mice were initially reported to be resistant to excitotoxic damaged caused by kainic acid (Schauwecker and Steward, 1997); however, our use of this "resistant" strain in stress-related work evaluating GFAP levels by ELISA revealed elevated protein levels, and therefore, a glial response to apparent neuronal damage. To understand this discrepancy, we conducted dose-response and time-course analyses of intoxication in this murine strain. KA-induced changes in hippocampal neuroanatomy and subsequent induction of reactive gliosis and damage to the blood–brain barrier in C57BL/6J mice recently have been described (Benkovic et al., 2004). Here, we report regional neuropathological changes in adult and aged mice treated systemically with KA and subsequently analyzed histologically with the cupric-silver neurodegeneration stain. Although we observed inter-animal variation in the extent of damage, mice of both ages displayed consistent regional pathology following treatment. In adult mice, KA-induced argyrophilia was generally restricted to grey matter; however, in aged mice, silver deposition was observed on fibers in several white matter tracts.

The resistance of C57BL/6 mice to KA-induced neuropathology was originally postulated to be a consequence of route of administration: systemic subcutaneous injection failed to produce neuropathology (Araki et al., 2002; Schauwecker, 2003; Schauwecker and Steward, 1997); however, intraventricular (Schauwecker, 2002) or intraamygdaloid (Araki et al., 2002) administration caused neuronal damage. In contrast, several laboratories evaluating C57BL/6 mice treated with KA by systemic intraperitoneal or intranasal application and analyzed by Nissl or Fluoro-Jade B staining have reported damage in hippocampal subregions CA1 and/or CA3 (Benkovic et al., 2004; Chen et al., 2002, 2004a,b; Hu et al., 1998; Royle et al., 1999; Sriram et al., 2002). In our previous evaluations of the time-course of KA-induced neuropathology, two important concepts emerged: sensitive indicators of damage revealed neuropathology not observed by traditional histological stains (Nissl and H&E); and damage must be evaluated over several time-points, both proximal and distal to treatment (Benkovic et al., 2004). In sequential brain sections from KA treated mice, we observed considerable neuropathology revealed by the cupric-silver neurodegeneration stain and Fluoro-Jade B, and Nissl stains that generally failed to show neuropathology. Because of the high packing density of neurons in hippocampus, small alterations in cell number are probably undetectable by Nissl staining unless stereological counting methods are incorporated (West et al., 1991). Utilization of standard histological stains and/or insufficient time-points following treatment may account for the reported resistance of C57BL/6 to KA-induced neurodegeneration.

KA-induced regional pathology has been extensively described in rat brain (Hopkins et al., 2000; Nadler et al., 1978; Olney et al., 1979; Schmued et al., 2005; Schwob et al., 1980; Sperk et al., 1983; Wang et al., 2005), and occurs with a temporal progression in hippocampus, thalamus, amygdala, neocortex, pyriform and olfactory cortices. Our C57BL/6J mice also show considerable sensitivity to kainic acid-induced damage in these regions. Neurons in the caudate nucleus were relatively spared in both rodents except for some scattered argyrophilia in the posterior putamen of rats, and minimal argyrophilia was observed in vivo in midbrain, pons, and cerebellum following a systemic injection (Schwob et al., 1980; Sperk et al., 1983). Argyrophilia in fiber tracts has been described in rat brain (Schwob et al., 1980); however, KA has been reported not to affect axons directly, but to cause initial damage to the cell body that is propagated to the processes (Divac et al., 1978; Olney and De Gubareff, 1978).

Excitotoxicity caused by KA can be propagated trans-synaptically. In rats, localized intraparenchymal or intrastriatal injection of kainic acid produced argyrophilia not only in primary target regions, but also in secondary regions receiving afferent projections from primary targets (Canudas et al., 2005; Chung et al., 1990; Krammer, 1980; Pearson et al., 1991; Schwob et al., 1980; Yasuda et al., 2001). In mice, we observed argyrophilia in hippocampal subfields CA1 and CA3, and the subiculum, which project to, and produced argyrophilia in the lateral septal nucleus. KA-damaged neurons in the hilus produced a band of argyrophilic terminals in the contralateral inner molecular layer of the dentate gyrus. Primary damage from entorhinal cortex neurons was transmitted through projections to hippocampal subregions CA1, CA3, and dentate gyrus, with terminal fibers in the stratum lacunosum-moleculare and the middle and outer molecular layers of the dentate gyrus displaying concomitant argyrophilia. The thalamus is a major relay center for multi-neuron pathways, and displayed a severe argyrophilic reaction in response to kainic acid-induced damage of several multi-neuron systems. The ability of KA to affect secondary targets suggests hyperexcitation of primary targets produces glutamatergic currents that are propagated trans-synaptically causing physiological damage to neurons receiving afferent projections from principal targets (Ben-Ari and Cossart, 2000; Ginsberg et al., 1999; Schwob et al., 1980).

The relationship between KA-induced EEG activity, behavioral seizures, and neurodegeneration remains controversial, and may be species-specific. In rats, a strict correlation is reported: neuropathology is consistently and positively correlated with tonic–clonic convulsions; animals not displaying behavioral seizures had no neuropathological deficits (Schwob et al., 1980; Zhang et al., 1998). In mice, the correlation is not as strict and may be dose-dependent: tonic–clonic seizure activity is positively correlated with high dosage (>25 mg/kg) KA intoxication in some (Chen et al., 2002; Hu et al., 1998; Schauwecker and Steward, 1997), but not all investigations (Araki et al., 2002; Benkovic et al., 2004; Chen et al., 2004a,b; Ferraro et al., 1995; Royle et al., 1999; Sriram et al., 2002). Experimental comparisons are complicated by differences in seizure scoring between laboratories. In our experimentation with animals purchased from Jackson Laboratories and treated with kainic acid (adult animals = 35 mg/kg, aged animals = 20 mg/kg), we observed two populations of seizing animals: mice which seized at stages 1–2 (which represents animals reported in this manuscript); and mice which seized at stage 5 and died. Brain EEG activity was measured and correlated to behavioral seizures in C57BL/6 mice treated with

KA (20 mg/kg) in an ongoing collaborative experiment that revealed status epilepticus in animals displaying stage 1 behavioral seizures (Dr. Hana Kubova, unpublished observation). These results have been confirmed in recent reports (Arabadzisz et al., 2005; Mazarati et al., 2004) and have led to the description of a state of "non-convulsive status epilepticus" in KA-treated mice (Arabadzisz et al., 2005). In mice, it seems likely that status epilepticus can be reflected by behavioral seizures of less than tonic–clonic severity, and that KA-induced neuronal damage is more a consequence of animals achieving status epilepticus than tonic–clonic seizures. Since we observed significant argyrophilia in mice of both ages which generally seized at stage 1, we conclude tonic–clonic seizure activity is not a prerequisite for neuropathology in C57BL/6J mice.

The genetic and/or physiological properties which regulate neuronal sensitivity to KA-induced excitotoxic damage remain speculative. In our regional analysis of neuropathology, we observed brain nuclei displaying severe argyrophilia located adjacent to regions appearing relatively normal. Even more perplexing is the relative lack of apparent neuropathology in entire brain regions such as cerebellum and pons. Explanations are speculative and concentrate on differences between populations of neurons with respect to the mechanisms by which KA may cause neurodegeneration, i.e., exacerbation of glutamate release, excessive activation of synaptic inputs, differential expression of KA receptor subtypes (and the effect on calcium mobilization), and modulation of inhibitory GABA potentials (reviewed in (Ben-Ari and Cossart, 2000)). It also seems reasonable that several mechanisms may operate simultaneously.

Age of the experimental animals at the time of treatment is a variable that impacts the pathological response to excitotoxicity in certain brain regions. At the earliest time-point analyzed, aged animals displayed argyrophilic neurons throughout all hippocampal regions while adult animals showed less damage that was restricted to subpopulations of hippocampal neurons. In contrast, cortical regions displayed argyrophilia earlier in adults than in aged animals. The hippocampus of aged animals appears to exhibit increased sensitivity to KA; however, the possibility remains that other brain regions of aged mice appear less sensitive than adults since they received less total KA. In animals of both ages, argyrophilia in amygdaloid regions was considerably less than in hippocampus at the earliest time-point examined, but roughly equivalent by 24 h post-treatment suggesting that amygdaloid argyrophilia is a combination of direct damage to amygdaloid neurons, and secondary damage from other principal targets that project to amygdaloid nuclei.

Regional patterns of pathology revealed by the various histological stains utilized in this investigation were overlapping, i.e., areas displaying KA-induced argyrophilia also displayed astroglial and microglial activation. Argyrophilic brain regions were consistent between adult and aged animals; however, the glial response was greater in aged animals suggesting that the response was either/both a consequence of greater damage, or that the regulation of the magnitude and time-course of argyrophilia and subsequent return to baseline was affected by age (i.e., altered dose–response characteristics). In the microenvironment, damage signals emanating from neurons, and cytokines released from activated glial cells are subject to the kinetics of diffusion that result in properly localized regions of gliosis (Sriram and O'Callaghan, 2005). Microglial cells have been implicated in the activation of astrocytes; however, our earliest time-point of 12 h post-treatment was not early enough to reveal temporal activation of the two types of glial cells. Astrocytes can also respond to subtle neuronal damage directly without intervening microglial involvement (Sriram and O'Callaghan, 2005). This independent astroglial activation may account for the increased basal GFAP immunoreactivity in saline-injected aged animals in response to an age-related degeneration of nerve terminals that also produces low-level regional argyrophilia (Bronson et al., 1993; O'Callaghan and Miller, 1991), or may reflect altered basal regulation of astrocytes with age (Nichols et al., 2001; O'Callaghan and Miller, 1991).

Our results indicate the C57BL/6J mouse is susceptible to excitotoxic damage induced by systemic injection of KA, and that aged animals have increased sensitivity to intoxication. We emphasize the necessity for histopathological analysis of potentially neurotoxic compounds utilizing sensitive indicators of neurodegeneration such as cupric-silver evaluated over a time-course both proximal and distal following treatment. These guidelines have enabled us to observe considerable argyrophilia in mice which have displayed mild KA-induced seizure activity indicating neurodegenerative changes in the absence of tonic–clonic convulsions.

4. Experimental procedures

4.1. *Animals*

Male C57BL/6J mice were purchased from Jackson Laboratories and were group-housed on a 12/12 light/dark cycle with access to food and water ad libitum, and allowed to age to 20 months in the vivarium of the West Virginia University in accordance with the guidelines of the Institutional Animal Care and Use Committee (IACUC). A second set of mice was purchased from Jackson Laboratories and aged to four months in the vivarium of CDC-NIOSH under the guidelines established by the Animal Care and Use Committee (ACUC).

4.2. *Dosing regimen*

Adult mice were injected intraperitoneally (i.p.) with 35 mg/kg kainic acid (Sigma), while aged mice were treated with 20 mg/kg in order to prevent excessive mortality in a numerically finite colony. An additional group of adult animals received the same dose as the aged animals in order to compare the magnitude of reactive gliosis as a function of age. KA was introduced before 12:00 P.M. in order to avoid synergistic interactions with circadian fluctuations in hormones and neurotransmitters (Roberts and Keith, 1994), and induced seizures were scored for 4 h post-injection according to the Racine scale using the following criteria: stage 1—mouth and facial movements; stage 2—head nodding; stage 3—forelimb clonus; stage 4—rearing; stage 5—rearing and falling (Racine, 1972).

4.3. *Tissue collection and processing for ELISA*

Mice were killed by decapitation 7 days following treatment, and the brains were rapidly removed and bisected. The hippocampus was dissected free-hand on a cold plate (Model TCP-2, Sigma-Aldrich) for subsequent determination of GFAP by ELISA. Samples

were weighed, immediately frozen on dry ice, and stored at –70 °C until analyzed.

4.4. GFAP ELISA

Hippocampal samples were sonified in 10 volumes hot 1% SDS (Sigma) and total protein was determined by the BCA method (Smith et al., 1985). GFAP concentration was assayed using a sandwich ELISA (O'Callaghan, 1991; O'Callaghan, 2002).

4.5. Tissue collection and processing for histology

Mice were allowed to recover for 12 h, 1 day, 3 days, or 7 days following KA treatment, were deeply anesthetized with Sleepaway (Fort Dodge Animal Health), and were perfused transcardially with 100 ml wash solution (0.8% w/v sodium chloride, 0.4% w/v dextrose, 0.8% w/v sucrose, 0.023% w/v anhydrous calcium chloride, 0.025% w/v anhydrous sodium cacodylate in deionized water) followed by 150 ml perfusion solution (4.0% w/v sucrose, 4.0% w/v paraformaldehyde, 1.072% w/v anhydrous sodium cacodylate in deionized water). Brains were allowed to harden in the skull for 7 days, were removed, stored in fixative, and delivered to NeuroScience Associates (NSA, Knoxville, TN) as coded samples for sectioning and staining. At NSA, 16 brains (n = 3–4 per group) were group embedded in a gelatin matrix using MultiBrain™ technology, frozen in isopentane, sectioned in the horizontal plane at 35 μm on an AO860 sliding microtome, and collected into 4.0% formaldehyde containing 4.2% sodium cacodylate (pH 7.2). MultiBrain™ technology allows simultaneous sectioning of control and treated brains and maximizes uniform staining across specimens. Time-course intervals for histology were based on previous experimentation which revealed KA-induced damage in adult C57BL/6J mice by 12 h following treatment (Benkovic et al., 2000).

4.6. Cupric-silver neurodegeneration stain

Every sixth section was stained with the cupric-silver neurodegeneration stain using an adaptation of the original procedure (de Olmos et al., 1994). Sections cut from the MultiBrain™ block were collected free-floating, rinsed in PBS, and placed in an aqueous mixture of silver nitrate, copper nitrate, cadmium nitrate, pyridine, and ethanol. Sections were subsequently processed through the following sequence: acetone; silver nitrate in combination with ammonium and sodium hydroxide; and a weak formaldehyde-citric acid and ethanol solution (for reduction). Following a PBS rinse, sections were bleached in potassium ferricyanide and sodium borate to remove unreduced silver. Following several rinses, sections were mounted on 2 × 3 in. glass slides, were air dried, and coverslipped.

4.7. GFAP immunohistochemistry

To visualize GFAP immunoreactivity, sections cut from the MultiBrain™ block were stained free-floating. Following hydrogen peroxide treatment and blocking serum, sections were immunostained with a 1:2000 dilution of primary polyclonal rabbit anti-cow GFAP antibody (Dako), a goat anti-rabbit secondary antibody, and an avidin–biotin–HRP complex (Vector Laboratories). Incubation times were 24 h at 4 °C for the primary antibody, 30 min at room temperature (RT) for the secondary antibody, and 1 h at RT for the avidin–biotin–HRP complex. Sections were treated with diaminobenzidine tetrahydrochloride (DAB, Sigma), rinsed, mounted on gelatinized (subbed) glass slides, air dried, and coverslipped.

4.8. Lectin staining

Microglial cells were visualized by staining with *Griffonia simplicifolia* Isolectin B4 (IsoB4, Vector Laboratories Inc.) using a modified procedure (McCann et al., 1996). Free-floating sections were rinsed and incubated overnight at 4 °C in biotinylated-lectin diluted to 10 μg/ml in DPBS containing divalent cations (0.1 mM calcium chloride, 0.1 mM magnesium chloride). Sections were rinsed, incubated with tertiary ABC complex for 1 h at RT, rinsed, reacted with DAB (25 mg/50 ml DPBS + 50 μl 30% hydrogen peroxide), rinsed, mounted onto 75 × 50 mm microscope slides, air dried, and coverslipped.

4.9. IgG staining procedure

Localization of IgG was achieved following an abbreviated immunostaining protocol using a Mouse Vectastain Elite ABC kit (PK-6102, Vector Laboratories). Free-floating sections were rinsed in DPBS and transferred directly to secondary antibody solution diluted in DPBS (1:1000 in the absence of serum) for 2 h at RT. Following DPBS rinses, sections were incubated with tertiary ABC complex for 1 h at RT. Sections were washed, reacted with DAB (25 mg/50 ml DPBS + 50 μl 30% hydrogen peroxide (Sigma)), rinsed, mounted onto 75 × 50 mm microscope slides, air dried, and coverslipped. Additional slides were counterstained with hematoxylin.

4.10. Regional histological analysis

Sequential horizontal sections were analyzed for KA-induced neuropathology in various regions in the dorsal to ventral direction. Brain regions showing KA-induced argyrophilia were identified and delineated by comparison to the C57BL/6 mouse brain atlas (Sidman et al., 1971).

4.11. Microscopic analysis

Microscopy of stained sections was performed at CDC-NIOSH on an Olympus BX-50 microscope interfaced with a Spot II digital camera controlled by a Macintosh G4 computer. Images were captured with Spot software (v3.0.5), assembled and labeled in Adobe Photoshop 6.0, and printed on a Codonics graphics printer (NP-1600).

4.12. Pathology scoring

Slides were scored blindly for severity of argyrophilia revealed by the cupric-silver neurodegeneration stain using a semi-quantitative four-point rating scale: 0 = no pathology; 1 = mild pathology; 2 = moderate pathology; 3 = severe pathology.

4.13. Statistical analysis

Mean GFAP levels and associated standard errors were computed using one way ANOVA using JMP (SAS Institute Inc.). Differences between means were analyzed by the Student's t test, and were considered different when probability values were less than 0.05.

Mean pathological scores and associated standard errors for hippocampal subregions of individual animals were computed using JMP (SAS Institute Inc.). Data were analyzed using a one-way non-parametric Wilcoxon/Kruskal–Wallis ANOVA, and differences in means were considered different when Prob>ChiSq values were less than 0.05.

REFERENCES

Arabadzisz, D., Antal, K., Parpan, F., Emri, Z., Fritschy, J.M., 2005. Epileptogenesis and chronic seizures in a mouse model of temporal lobe epilepsy are associated with distinct EEG patterns and selective neurochemical

alterations in the contralateral hippocampus. Exp. Neurol. 194, 76–90.
Araki, T., Simon, R.P., Taki, W., Lan, J.Q., Henshall, D.C., 2002. Characterization of neuronal death induced by focally evoked limbic seizures in the C57BL/6 mouse. J. Neurosci. Res. 69, 614–621.
Ben-Ari, Y., Cossart, R., 2000. Kainate, a double agent that generates seizures: two decades of progress. TINS 23, 580–587.
Benkovic, S.A., O'Callaghan, J.P., Miller, D.B., 2000. Impact of the stress hormone corticosterone on hippocampal response to neurotoxic injury in susceptible and resistant mouse strains. Society for Neuroscience Annual Meeting, New Orleans, p. 856.18.
Benkovic, S.A., O'Callaghan, J.P., Miller, D.B., 2004. Sensitive indicators of injury reveal hippocampal damage in C57BL/6J mice treated with kainic acid in the absence of tonic–clonic seizures. Brain Res. 1024, 59–76.
Bowyer, J.F., Peterson, S.L., Rountree, RL., Tor-Agbidye, J., Wang, G.J., 1998. Neuronal degeneration in rat forebrain resulting from D-amphetamine-induced convulsions is dependent on seizure severity and age. Brain Res. 809, 77–90.
Bronson, R.T., Lipman, R.D., Harrison, D.E., 1993. Age-related gliosis in the white matter of mice. Brain Res. 609, 124–128.
Canudas, A.M., Pezzi, S., Canals, J.M., Pallas, M., Alberch, J., 2005. Endogenous brain-derived neurotrophic factor protects dopaminergic nigral neurons against transneuronal degeneration induced by striatal excitotoxic injury. Mol. Brain Res. 134, 147–154.
Cass, W.A., Peters, L.E., Smith, M.P., 2005. Reductions in spontaneous locomotor activity in aged male, but not female, rats in a model of early Parkinson's disease. Brain Res. 1034, 153–161.
Chen, Z., Ljunggren, H.-G., Bogdanovic, N., Nennesmo, I., Winblad, B., Zhu, J., 2002. Excitotoxic neurodegeneration induced by intranasal administration of kainic acid in C57BL/6 mice. Brain Res. 931, 135–145.
Chen, Z., Ljunggren, H.-G., Zhu, S.-W., Winblad, B., Zhu, J., 2004a. Reduced susceptibility to kainic acid-induced excitotoxicity in T-cell deficient CD4/CD8(–/–) and middle-aged C57BL/6 mice. J. Neuroimmunol. 146, 33–38.
Chen, z., Yu, S., Concha, H.Q., Zhu, Y., Mix, E., Winblad, B., Ljunggren, H.G., Zhu, J., 2004b. Kainic acid-induced excitotoxic hippocampal neurodegeneration in C57/BL/6 mice: B cell and T cell subsets may contribute differently to the pathogenesis. Brain Behav. Immun. 18, 175–185.
Chung, S.K., Cohen, R.S., Pfaff, D.W., 1990. Transneuronal degeneration in the midbrain central gray following chemical lesions in the ventromedial nucleus: a qualitative and quantitative analysis. Neuroscience 38, 409–426.
Dawson Jr., R., Wallace, D.R., 1992. Kainic acid-induced seizures in aged rats: neurochemical correlates. Brain Res. Bull. 29, 459–468.
de Olmos, J.S., Beltramino, C.A., de Olmos de Lorenzo, S., 1994. Use of an amino-cupric-silver technique for the detection of early and semiacute neuronal degeneration caused by neurotoxicants, hypoxia, and physical trauma. Neurotox. Teratol. 16, 545–561.
Divac, I., Markowitsch, H.J., Pritzel, M., 1978. Behavioral and anatomical consequences of small intrastriatal injections of kainic acid in the rat. Brain Res. 151, 523–532.
Eng, L.G., Ghirnikar, R.S., Lee, Y.L., 2000. Glial fibrillary acidic protein: GFAP-thirty-one years (1969–2000). Neurochem. Res. 25, 1439–1451.
Ferraro, T.N., Golden, G.T., Smith, G.G., Berrettini, W.H., 1995. Differential susceptibility to seizures induced by systemic kainic acid treatment in mature DBA/2J and C57BL/6J mice. Epilepsia 36, 301–307.
Ginsberg, S.D., Portera-Cailliau, C., Martin, L.J., 1999. Fimbria–fornix transfection and excitotoxicity produce similar neurodegeneration in the septum. Neuroscience 88, 1059–1071.
Hopkins, K.J., Guang-Jian, W., Schmued, L.C., 2000. Temporal progression of kainic acid induced neuronal and myelin degeneration in the rat forebrain. Brain Res. 864, 69–80.
Hu, R.Q., Koh, S., Torgerson, T., Cole, A.J., 1998. Neuronal stress and injury in C57/BL mice after systemic kainic acid administration. Brain Res. 810, 229–240.
Imam, S.Z., Ali, S.F., 2001. Aging increases the susceptiblity to methamphetamine-induced dopaminergic neurotoxicity in rats: correlation with peroxynitrite production and hyperthermia. J. Neurochem. 78, 952–959.
Krammer, E.B., 1980. Anterograde and transsynaptic degeneration 'en cascade' in basal ganglia induced by intrastriatal injection of kainic acid: an animal analogue of Huntington's disease. Brain Res. 196, 209–221.
Little, A.R., O'Callaghan, J.P., 2002. The astrocyte response to neural injury: a review and reconsideration of key features. In: Lester, D., Slikker, W., Lazarovici, P. (Eds.), Site-Specific Neurotoxicity. Tayler and Francis Publishers, London, pp. 233–265.
Mazarati, A., Lu, X., Shinmei, S., Badie-Mahdavi, H., Bartfai, T., 2004. Patterns of seizures, hippocampal injury and neurogenesis in three models of status epilepticus in galanin receptor type 1 (GALR1) knockout mice. Neuroscience 128, 431–441.
McCann, M.J., O'Callaghan, J.P., Martin, P.M., Bertram, T., Streit, W.J., 1996. Differential activation of microglia and astrocytes following trimethyl tin-induced neurodegeneration. Neuroscience 72, 273–281.
Miller, D.B., O'Callaghan, J.P., Ali, S.F., 2000. Age as a susceptibility factor in the striatal dopaminergic neurotoxicity observed in the mouse following substituted amphetamine exposure. Ann. N. Y. Acad. Sci. 914, 194–207.
Nadler, J.V., Perry, B.W., Cotman, C.W., 1978. Intraventricular kainic acid preferentially destroys hippocampal pyramidal cells. Nature 271, 676–677.
Nichols, N.R., Zieba, M., Bye, N., 2001. Do glucocorticoids contribute to brain aging? Brain Res. Rev. 37, 273–286.
Norenberg, M.D., 1994. Astrocyte responses to CNS injury. J. Neuropathol. Exp. Neurol. 53, 213–220.
O'Callaghan, J.P., 1991. Quantification of glial fibrillary acidic protein: comparison of slot immunobinding assays with a novel sandwich ELISA. Neurotoxicol. Teratol. 13, 275–281.
O'Callaghan, J.P., 1993. Quantitative features of reactive gliosis following toxicant-induced damage of the CNS. Ann. N. Y. Acad. Sci. 679, 195–210.
O'Callaghan, J.P., 2002. Measurement of glial fibrillary acidic protein. In: Costa, L.G. (Ed.), Current Protocols in Toxicology. John Wiley and Sons, New York, pp. 12–12.81.1.
O'Callaghan, J.P., Miller, D.B., 1991. The concentration of glial fibrillary acidic protein increases with age in the mouse and rat brain. Neurobiol. Aging 12, 171–174.
O'Callaghan, J.P., Miller, D.B., 1994. Neurotoxicity profiles of substituted amphetamines in the C57BL/6J mouse. J. Pharmacol. Exp. Ther. 270, 741–751.
Olney, J.W., De Gubareff, T., 1978. The fate of synaptic receptors in the kainate-lesioned striatum. Brain Res. 140, 340–343.
Olney, J.W., Fuller, T., De Gubareff, T., 1979. Acute dendrotoxic changes in the hippocampus of kainate treated rats. Brain Res. 176, 91–100.
Panickar, K.S., Norenberg, M.D., 2005. Astrocytes in cerebral ischemic injury: morphological and general considerations. Glia 50, 287–298.
Pearson, H.E., Sonstein, W.J., Stoffler, D.J., 1991. Selectivity of kainic acid as a neurotoxin within the dorsal lateral geniculate nucleus of the cat: a model for transneuronal retrograde degeneration. J. Neurocytol. 20, 376–386.

Perl, T.M., Bedard, L., Kosatsky, T., Hockin, J.C., Todd, E.C., Remis, R.S., 1990. An outbreak of toxic encephalopathy from eating mussels contaminated with domoic acid. N. Engl. J. Med. 322, 1775–1780.

Petzold, A., Baker, D., Pryce, G., Keir, G., Thompson, E.J., Giovannoni, G., 2003. Quantification of neurodegeneration by measurement of brain-specific proteins. J. Neuroimmunol. 138, 45–48.

Racine, R.J., 1972. Modification of seizure activity by electrical stimulation: II. Motor seizure. Electroencephalogr. Clin. Neurophysiol. 32, 281–294.

Roberts, A.J., Keith, L.D., 1994. Sensitivity of the circadian rhythm of kainic acid-induced convulsion susceptibility to manipulations of corticosterone levels and mineralocorticoid receptor binding. Neuropharmacology 33, 1087–1093.

Royle, S.J., Collins, F.C., Rupniak, H.T., Barnes, J.C., Anderson, R., 1999. Behavioural analysis and susceptibility to CNS injury of four inbred strains of mice. Brain Res. 816, 337–349.

Sankar, R., Blossom, E., Clemons, K., Charles, P., 1983. Age-associated changes in the effects of amphetamine on the blood–brain barrier of rats. Neurobiol. Aging 4, 65–68.

Santos, J.B., Schauwecker, P.E., 2003. Protection provided by cyclosporin A against excitotoxic neuronal death is genotype dependent. Epilepsia 44, 995–1002.

Scallet, A.C., Pothuluri, N., Rountree, R.L., Matthews, J.C., 2000. Quantitating silver-stained neurodegeneration: the neurotoxicity of trimethyltin (TMT) in aged rats. J. Neurosci. Methods 98, 69–76.

Schauwecker, P.E., 2002. Modulation of cell death by mouse genotype: differential vulnerability to excitatory amino acid-induced lesions. Exp. Neurol. 178, 219–235.

Schauwecker, P.E., 2003. Differences in ionotropic glutamate receptor subunit expression are not responsible for strain-dependent susceptibility to excitotoxin-induced injury. Mol. Brain Res. 112, 70–81.

Schauwecker, P.E., Steward, O., 1997. Genetic determinants of susceptibility to excitotoxic cell death: Implications for gene targeting approaches. Proc. Natl. Acad. Sci. 94, 4103–4108.

Schmued, L.C., Stowers, C.C., Scallet, A.C., Xu, L., 2005. Fluoro-Jade C results in ultra high resolution and contrast labeling of degenerating neurons. Brain Res. 1035, 24–31.

Schwob, J.E., Fuller, T., Price, J.L., Olney, J.W., 1980. Widespread patterns of neuronal damage following systemic or intracerebral injections of kainic acid: a histological study. Neuroscience 5, 991–1014.

Sidman, R.L., Angevine, J.B.J., Taber Pierce, E., 1971. Atlas of the Mouse Brain and Spinal Cord. Harvard Univ. Press, Cambridge.

Skaper, S.D., Floreani, M., Ceccon, M., Facci, L., Giusti, P., 1999. Excitotoxicity, oxidative stress, and the neuroprotective potential of melatonin. Ann. N. Y. Acad. Sci. 890, 107–118.

Smith, P.K., Krohn, R.I., Hermanson, G.T., Mallia, A.K., Gartner, F.H., Provenzano, M.D., Fujimoto, E.K., Goeke, N.M., Olson, B.J., Klenk, D.C., 1985. Measurement of protein using bicinchoninic acid. Anal. Biochem. 150, 76–85.

Sperk, G., Lassmann, H., Baran, H., Kish, S.J., Seitelberger, F., Hornykiewicz, O., 1983. Kainic acid induced seizures: neurochemical and histopathological changes. Neuroscience 10, 1301–1315.

Sriram, K., O'Callaghan, J.P., 2005. Signaling mechanisms underlying toxicant-induced gliosis. In: Aschner, M., Costa, L.G. (Eds.), The Role of Glia in Neurotoxicity. CRC Press, Boca Raton, pp. 141–171.

Sriram, K., Benkovic, S.A., Miller, D.B., O'Callaghan, J.P., 2002. Obesity exacerbates chemically induced neurodegeneration. Neuroscience 115, 1335–1346.

Wang, Q., Yu, S., Simonyi, A., Sun, G.Y., Sun, A.Y., 2005. Kainic acid-mediated excitotoxicity as a model for neurodegeneration. Mol. Neurobiol. 31, 3–16.

West, M.J., Slomianka, L., Gundersen, H.J.G., 1991. Unbiased stereological estimation of the total number of neurons in the subdivisions of the rat hippocampus using the optical fractionator. Anat. Rec. 231, 482–497.

Wozniak, D.F., Stewart, G.R., Miller, J.P., Olney, J.W., 1991. Age-related sensitivity to kainate neurotoxicity. Exp. Neurol. 114, 250–253.

Wuerthele, S.M., Lovell, K.L., Jones, M.Z., Moore, K.E., 1978. A histological study of kainic acid-induced lesions in the rat brain. Brain Res. 149, 489–497.

Yang, J., Houk, B., Shah, J., Hauser, K.F., Luo, Y., Smith, G., Schauwecker, E., Barnes, G.N., 2005. Genetic background regulates semaphorin gene expression and epileptogenesis in mouse brain after kainic acid status epilepticus. Neuroscience 131, 853–869.

Yasuda, H., Fujii, M., Fujisawa, H., Ito, H., Suzuki, M., 2001. Changes in nitric oxide synthesis and epileptic activity in the contralateral hippocampus of rats following intrahippocampal kainate injection. Epilepsia 42, 13–20.

Zhang, J.W., Deb, S., Gottschall, P.E., 1998. Regional and differential expression of gelatinases in rat brain after systemic kainic acid or bicuculline administration. Eur. J. Neurosci. 10, 3358–3368.